



# Ag<sub>m</sub>Rh<sub>n</sub> clusters with $m + n \leq 55$

Nicolas Louis<sup>1</sup> · Stephan Kohaut<sup>1</sup> · Michael Springborg<sup>1</sup>

Received: 4 October 2020 / Accepted: 8 March 2021 / Published online: 30 March 2021  
© The Author(s) 2021

## Abstract

Using a combination of genetic algorithms for the unbiased structure optimization and a Gupta many-body potential for the calculation of the energetic properties of a given structure, we determine the putative total-energy minima for all Ag<sub>m</sub>Rh<sub>n</sub> clusters with a total number of atoms  $m + n$  up to 55. Subsequently, we use various descriptors to analyze the obtained structural and energetic properties. With the help of a similarity function, we show that the pure Ag and Rh clusters are structurally similar for sizes up to around 20 atoms. The same approach gives that the mixed clusters tend to possess a larger structural similarity with the pure Rh clusters than with the pure Ag clusters. However, for clusters with  $m \simeq n \geq 25$ , other structures dominate. The effective coordination numbers for the Ag and Rh atoms as well as the radial distributions of those atoms indicate that there is a tendency towards segregation with Rh atoms forming an inner part and the Ag atoms forming a shell. Only few clusters, all with a fairly large total number of atoms, are found to be particularly stable.

**Keywords** Bimetallic clusters · Unbiased structure optimization · Energetic properties · Structural properties

## 1 Introduction

For some few decades, there has been an intense interest in the properties of clusters/nanoparticles made up of metal atoms. One of the studies that initiated the current interest is due to Knight et al. [1] who studied mass abundance spectra of clusters made up of sodium atoms and used a simple jellium model to explain the unexpected result that the abundance showed a marked size dependence. This example demonstrates very clearly the reason for the interest in these nanoparticles: Their size is below that of the thermodynamic limit so that their properties as a function of size do not follow simple scaling laws. Since then there has appeared very many experimental and theoretical studies of the properties of monatomic, metallic clusters. Also the person to whom this paper is devoted, Fernand Spiegelmann, has made excellent, theoretical contributions to this field.

Exactly the fact that these nanoparticles have sizes below the thermodynamic limit makes it interesting and relevant

to explore and eventually also exploit their properties. However, for theoretical studies this is very often connected with a serious challenge: in order to study the properties, it is most often necessary to know the structure of the nanoparticles which may be (very) different from that of the crystalline material. In addition, it is known that for a cluster A<sub>n</sub> with  $n$  identical atoms, the number of inequivalent, (meta-) stable structures scales non-polynomial, i.e., exponential with  $n$ , so that the identification of the structure of the global total-energy minimum becomes extremely difficult.

Even further flexibility can be obtained by considering bimetallic clusters A<sub>m</sub>B<sub>n</sub> (see, e.g., [2]). Here, the existence of so-called homotops [3, 4], i.e., isomers with the same overall structure but differing in the arrangement of the A and B atoms, leads to additional complications from a theoretical point of view since the number of (meta-)stable structures thereby grows by the factor  $\binom{m+n}{m}$ . On the other hand, bimetallic systems of reduced dimensionality may possess phase diagrams that differ from those of the solid counterparts, as has been shown for, e.g., surface alloys [5]. Therefore, also bimetallic clusters (nanoalloys) may possess unexpected properties that are unmatched by their macroscopic counterparts and that may be exploited for applications.

As an example, we shall in the present work study the energetic and structural properties of Ag<sub>m</sub>Rh<sub>n</sub> clusters with a total number of atoms  $m + n$  up to 55. Silver and rhodium are

Published as part of the special collection of articles “Festschrift in honor of Fernand Spiegelmann”

✉ Michael Springborg  
m.springborg@mx.uni-saarland.de

<sup>1</sup> Physical and Theoretical Chemistry, University of Saarland, Campus B2.2, 66123 Saarbrücken, Germany

largely immiscible in the bulk. Thus, more than 100 years ago, Rossler reported a very small solubility of rhodium in silver [6] whereas a larger solubility of silver in rhodium is found that, furthermore, increases with temperature from 4.7 atom% at room temperature to around 19 atom% at 1200°C [7]. This makes it very difficult to predict the behavior of the two metals when forming nanoalloys and it cannot be excluded that also in nanoalloys Ag and Rh are segregated. The purpose of the present work is to study this in more detail including whether a segregation takes place and, if so, what structures then result (e.g., Janus-particles or core-shell particles). In an earlier work [8] we studied this system for  $m + n \leq 20$  and  $n$  or  $m = 0, 1$ . Here, we shall extend that study to a much larger range of stoichiometries, i.e., considering all  $m + n \leq 55$ . This makes it necessary to change the computational approach slightly, as will be discussed in the next section. Section 3 contains the results and a discussion of those, whereas Sect. 4 summarizes our findings.

## 2 Computational method

In our earlier work on  $\text{Ag}_m\text{Rh}_n$  clusters we considered  $m + n \leq 20$  and  $m$  or  $n = 0, 1$  giving a total of 80 different systems. In the present work, the number of systems is much larger (1595) and most of the systems are in addition larger. An unbiased structure optimization using a high-level electronic-structure method is accordingly not possible due to computational costs. We shall, therefore, use a simpler description for the interatomic interactions that we also used partly in our earlier work [8].

For the calculation of the cohesive energy for a given structure and system, we use the Gupta many-body potential [9] as given by Rosato et al. [10] and according to which the total cohesive energy is given as

$$E_{\text{coh}} = \sum_i (E_{m,i} + E_{r,i}) \quad (1)$$

where the summation goes over all atoms of the system and with  $E_{m,i}$  and  $E_{r,i}$  being an attractive and a repulsive potential, respectively, for the  $i$ th atom. These are given as

$$E_{m,i} = - \left[ \sum_j \xi_j^2 e^{-2q_l(r_{ij}/r_l-1)} \right]^{1/2} \quad (2)$$

and

$$E_{r,i} = \sum_j A_l e^{-p_l(r_{ij}/r_l-1)}. \quad (3)$$

In these expressions,  $r_{ij}$  is the distance between atoms  $i$  and  $j$ ,  $r_l$  is the nearest-neighbor distance in the crystal lattice  $l$ , and  $p_l$ ,  $q_l$ ,  $\xi_j$ , and  $A_l$  are parameters. For the values of those

parameters, we use those given by Cleri and Rosatto [11] for Rh–Rh and Ag–Ag interactions and our own ones [8] for the Ag–Rh interactions.

As is evident, this approach does not include any explicit description of electronic degrees of freedom. In our earlier work [8] we combined this approach with a parameterized density-functional method that does include electrons explicitly. However, the number and sizes of the systems to be treated in the present work make such an approach computationally too demanding and, therefore, in the present work we have used only the Gupta potential.

For the unbiased structure optimization, we used genetic algorithms similar to what originally was proposed by Deaven and Ho [12] for cluster structure optimization. Thus, for each system we initially construct an even number of different structures randomly. These (so-called parents) are relaxed locally and subsequently separated into pairs. For each pair, a cutting and mating procedure is applied, whereby the two clusters are cut into two parts that are interchanged making sure that stoichiometry and size are unchanged. Also these so-called children are relaxed locally and out of the total set of parents and children, that half-part that has the lowest total energy is kept as the parents for the next generation. This is continued until the lowest total energy stays unchanged for many generations. In these calculations, also so-called mutations are included where random distortions of various kinds are applied.

## 3 Results

We shall repeatedly use the concept of a similarity function to quantify structural similarity between two clusters (or, eventually, also between a cluster and an infinite crystal). This function was described in some detail earlier [13] and shall, therefore, here be just briefly introduced.

When comparing two clusters, A and B with  $N_A$  and  $N_B$  atoms, respectively, we shall concentrate on the geometrical arrangement of the atoms and not take atom types into account. By scaling the coordinates of cluster B and translating and rotating the structure (and eventually also inverting the cluster in its center of mass), the resulting cluster B is placed on top of cluster A so that the quantity

$$q^2 = \frac{1}{2N} \left( \sum_{i=1}^N d^2(a_i, b(a_i)) + \sum_{i=1}^N d^2(b_i, a(b_i)) \right) \quad (4)$$

is minimized. Here, for each atom  $a_i$  in cluster A the closest atom  $b(a_i)$  in cluster B is identified and  $d(a_i, b(a_i))$  is their distance. Similarly, for every atom  $b_i$  in B, the closest atom  $a(b_i)$  in cluster A is identified and  $d(b_i, a(b_i))$  is their distance. Moreover,  $N$  is the smallest of  $N_A$  and  $N_B$ . Finally, from the smallest value of  $q^2$ , we calculate the similarity function

$$S = \frac{1}{1 + \frac{d}{u_i}} \quad (5)$$

where  $u_i$  is a unit length that is chosen as the average nearest-neighbor distance in cluster A.

Our experience is that two clusters are structurally similar if  $S > 0.9$  and dissimilar if  $S < 0.8$ .

Another quantity we shall consider is the average nearest-neighbor distance. For the determination of this, we use an approach due to Hoppe [14]. Thus, for the  $i$ th atom in a cluster with  $N$  atoms, the average bond length is defined as

$$d_{av}^i = \frac{\sum_{j=1}^N d_{ij} e^{[1-(d_{ij}/d_{av}^i)^6]}}{\sum_{j=1}^N e^{[1-(d_{ij}/d_{av}^i)^6]}} \quad (6)$$

with  $d_{ij}$  being the interatomic distance between atoms  $i$  and  $j$ . It is seen that  $d_{av}^i$  has to be determined iteratively. Subsequently, the average nearest-neighbor distance is calculated as the average of  $d_{av}^i$ ,

$$d_{av} = \frac{1}{N} \sum_{i=1}^N d_{av}^i. \quad (7)$$

From  $d_{av}^i$  also an effective coordination number ECN of atom  $i$  can be introduced,

$$ECN(i) = \sum_{j=1}^N e^{[1-(d_{ij}/d_{av}^i)^6]}. \quad (8)$$

Also in this case, we calculate an average effective coordination number,

$$ECN = \frac{1}{N} \sum_{i=1}^N ECN(i). \quad (9)$$

For the mixed  $Ag_mRh_n$  clusters, we may consider average effective coordination numbers for Ag and Rh, separately, by letting the sum in Eq. (9) run only over the Ag or Rh atoms and, correspondingly, dividing not with  $N$  but with  $m$  or  $n$ , respectively.

### 3.1 Pure clusters

We start the discussion of our results by considering the pure Ag and Rh clusters, also because these results shall be used as reference for the analysis of the mixed  $Ag_mRh_n$  clusters.

At first, we show in Fig. 1 the similarity function  $S$  for the comparison of the pure  $Ag_n$  and  $Rh_n$  clusters. It is seen that  $Ag_n$  and  $Rh_n$  are structurally very similar for  $n \leq 20$ , but that for larger values of  $n$  they become quite different with  $n = 33, 36, 38, 39, 42, 43, 54$  and  $55$  being exceptions. The different structures are often found when they are fragments of the 38- or 55-atomic icosahedra that are either differently

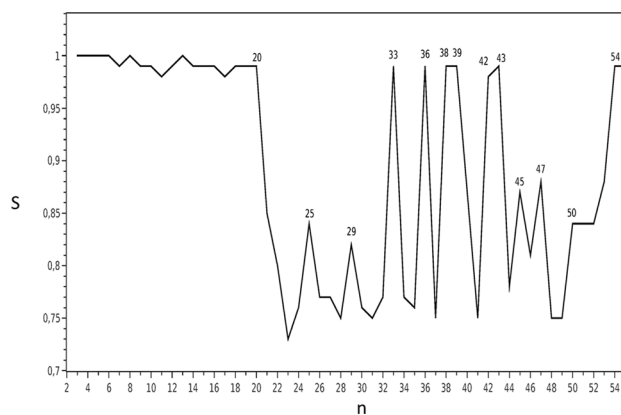


**Fig. 1** The similarity function for the comparison of the pure  $Ag_n$  clusters with the pure  $Rh_n$  clusters

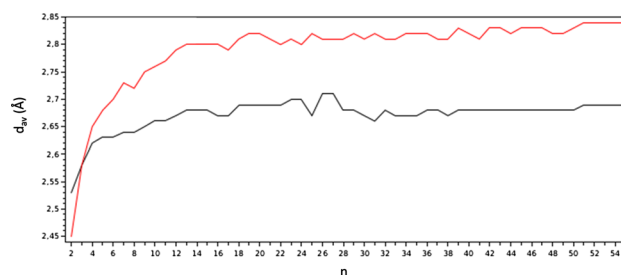


**Fig. 2** The average bond length according to Eqs. (6) and (7) of the pure  $Ag_n$  (red curve) and  $Rh_n$  (black curve) clusters

distorted ( $n = 21, 25$ ) or result as different fragments ( $n = 29, 45, 47, 50, 51, 52, 53$ ). In some cases, also different structural motifs are found for the clusters of the same size. Thus, for  $Rh_n$  but not for  $Ag_n$  for  $n = 31, 34$ , and  $35$  as well as for  $Ag_n$  but not for  $Rh_n$  for  $n = 41, 48$ , and  $49$ , structures based on the decahedron are found. In some few cases ( $Ag_{33}$ ,  $Ag_{37}$ ,  $Rh_{33}$ , and  $Rh_{38}$ ), we find a fragment of an octahedron as the most stable structure, in agreement with other studies.

Next, we show in Fig. 2 the average bond length as calculated using Eqs. (6) and (7). A convergence behavior can be identified, but even for the largest clusters the nearest-neighbor bond lengths of 2.89 Å and 2.75 Å for crystalline Ag and Rh, respectively, are not reached. This may not surprise when remembering that even for the largest clusters of the present study, most of the atoms are placed in lower-coordinated surface positions.

This can also be identified in Fig. 3 that shows the average effective coordination number according to Eqs. (8) and (9). It is interesting that the two curves lie so close to each other, but also that the number, 12, for the crystalline phases is far from being reached for the clusters of the size range of the present study.

Finally, we show in Fig. 4 the so-called stability function,

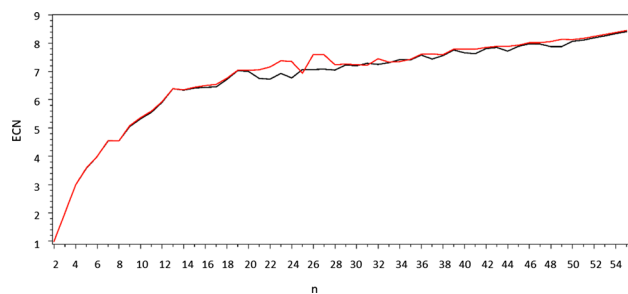


**Fig. 3** The average effective coordination number according to Eqs. (8) and (9) of the pure  $\text{Ag}_n$  (red curve) and  $\text{Rh}_n$  clusters (black curve)

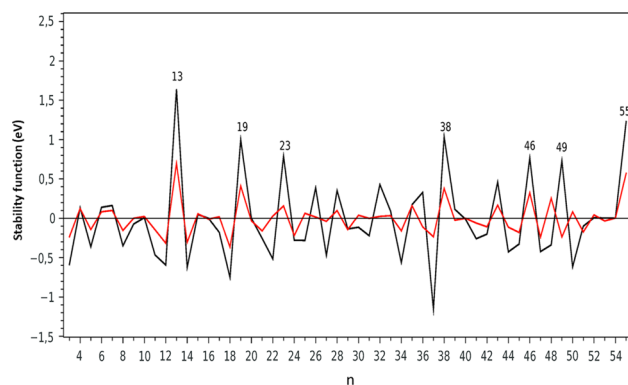


**Fig. 4** The stability function according to Eq. (10) of the pure  $\text{Ag}_n$  (red curve) and  $\text{Rh}_n$  (black curve) clusters

$$\Delta_2(n) = E_{\text{tot}}(n+1) + E_{\text{tot}}(n-1) - 2E_{\text{tot}}(n), \quad (10)$$

that compares the total energy of a given cluster size with those of the two neighboring sizes. Here,  $E_{\text{tot}}(k)$  is the total energy of the cluster with  $k$  atoms. Maxima in  $\Delta_2(n)$  correspond to particularly stable clusters and are often called magic clusters. In Fig. 4, we see that the present approach gives very similar stability functions for the two elements. This might be due to the simple form for the description of the interatomic interactions that is provided by the Gupta potential. Such approaches tend to predict that particularly compact, high-symmetric structures are particularly stable which indeed is the case for the magic sizes found here and that are marked in the figure.

### 3.2 Mixed clusters

When passing to the mixed  $\text{Ag}_m\text{Rh}_n$  clusters with  $m, n \neq 0$ , some of the questions we shall address include whether the two types of atoms will mix or segregate, whether the clusters resemble more the pure Ag or the pure Rh clusters, whether also in this case particularly stable clusters can be identified, and whether these are related to those of the pure clusters.

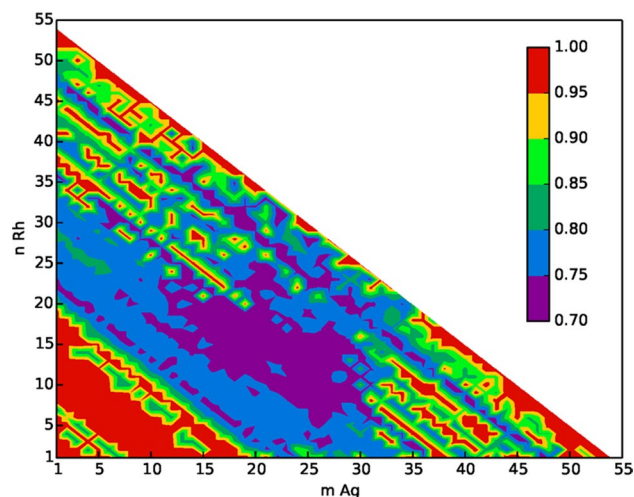


**Fig. 5** The similarity function for the comparison of the mixed  $\text{Ag}_m\text{Rh}_n$  clusters with the pure  $\text{Ag}_{m+n}$  clusters

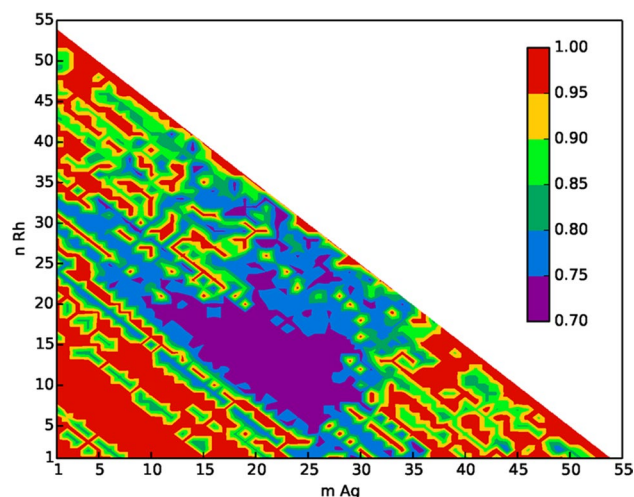


**Fig. 6** The similarity function for the comparison of the mixed  $\text{Ag}_m\text{Rh}_n$  clusters with the pure  $\text{Rh}_{m+n}$  clusters

At first we use the concept of similarity function to compare the structures of the mixed  $\text{Ag}_m\text{Rh}_n$  clusters with those of the pure  $\text{Ag}_{m+n}$  (Fig. 5) and pure  $\text{Rh}_{m+n}$  clusters (Fig. 6). It is seen that for  $m+n \leq 20$ , the mixed and the pure clusters are very similar, which partly is related to the fact that already the pure clusters are very similar (cf. Fig. 1). However, overall the mixed clusters of larger sizes tend to resemble more the pure Rh clusters than the pure Ag clusters. It is surprising that even the Ag-rich clusters have structures more similar to the pure Rh than to the pure Ag clusters. Thus, very few Rh atoms are required to make the overall structure similar to that of the pure Rh clusters.

From the average effective coordination numbers for the Ag and Rh atoms, separately, shown in Fig. 7, we see that Rh atoms are higher coordinated than Ag. As we shall

see further below, the mixed clusters show some tendency towards segregation so that the Rh atoms form an inner part and the Ag atoms an outer part. Thereby, it is obvious that Rh atoms have a higher coordination than Ag atoms.

A visual analysis of the structures of the mixed clusters suggests that many of those are based on the icosahedral structural motif. We can use the concept of similarity functions to quantify this further. Thus, we calculated the similarity function for the comparison of the structures of the mixed  $\text{Ag}_m\text{Rh}_n$  clusters with that of a 55-atom icosahedron, giving the results shown in Fig. 8. Indeed, it is seen that very many of the clusters have structures resembling a (part of an) icosahedron. Exceptions are clusters with  $m \approx n \geq 20$  and those with  $15 \leq n \leq 25$  and simultaneously  $m \leq 10$ .

Other structural motifs that are found for the mixed clusters include the octahedron that also was found for the pure clusters. In addition, we find many clusters with double- and

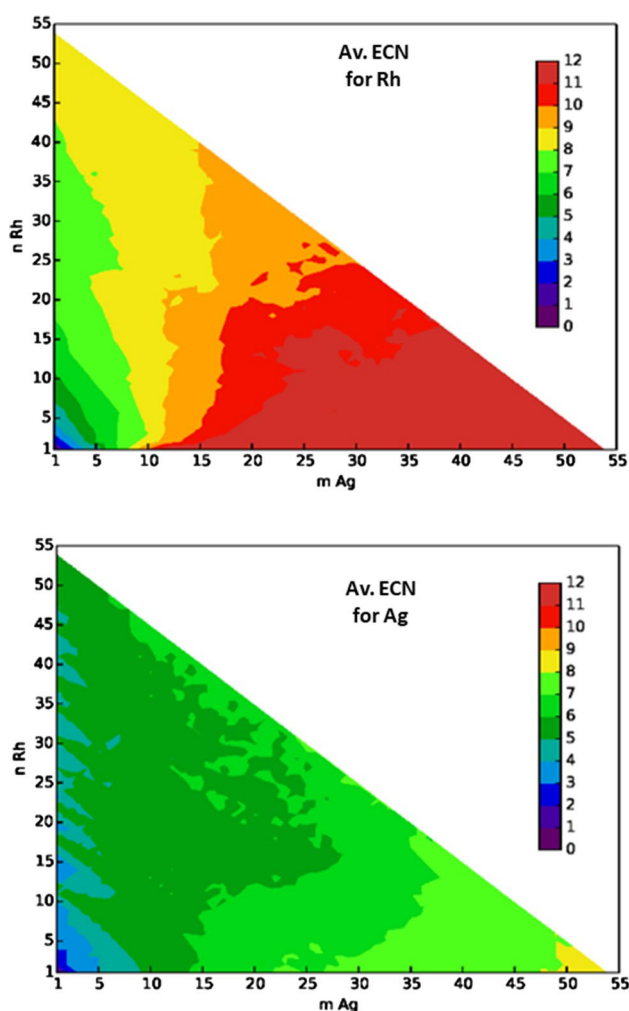


**Fig. 7** The average effective coordination number according to Eqs. (8) and (9) for the (upper part) Rh atoms and (lower part) Ag atoms in the mixed  $\text{Ag}_m\text{Rh}_n$  clusters

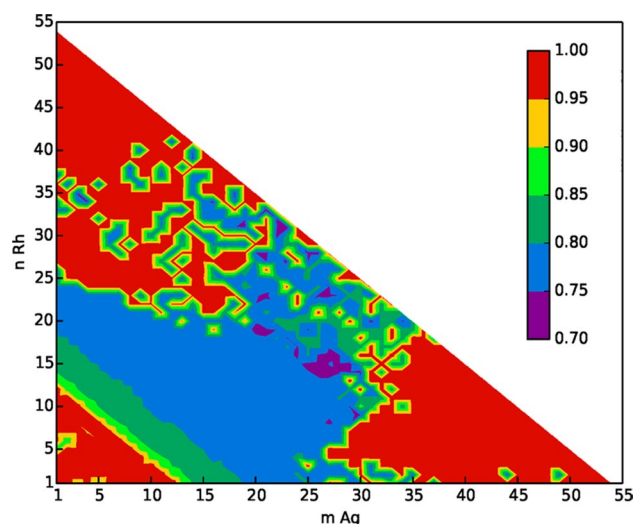


**Fig. 8** The similarity function for the comparison of the mixed  $\text{Ag}_m\text{Rh}_n$  clusters with an icosahedron with 55 atoms

polyicosahedral structures, in particular, for the clusters with  $m \approx n \geq 20$  and those with  $15 \leq n \leq 25$  and simultaneously  $m \leq 10$  that were mentioned above.

For the pure clusters, the stability function of Eq. (10) was very useful to identify sizes of particularly stable clusters. However, for the bimetallic clusters, it is less obvious how to define a similar function that is based on comparing the total energy of a given cluster size with those of neighboring sizes. We shall here consider the function

$$\Delta_2(m, n) = \frac{1}{8} \sum_{k,l=-1}^1 [E_{\text{tot}}(m+k, n+l) - E_{\text{tot}}(m, n)] \quad (11)$$

with  $E_{\text{tot}}(p, q)$  being the total energy of the  $\text{Ag}_p\text{Rh}_q$  cluster.

This function is shown in Fig. 9. Only few particularly stable clusters are identified, in particular such with a fairly large total number of atoms,  $m+n$ . Some interesting structures are found for clusters with  $m+n=34$ , for which  $\text{Ag}_{27}\text{Rh}_7$ ,  $\text{Ag}_{21}\text{Rh}_{13}$ ,  $\text{Ag}_{16}\text{Rh}_{18}$ , and  $\text{Ag}_9\text{Rh}_{25}$  are particularly stable clusters. It turns out that these clusters have a fairly high symmetry and mainly Rh atoms in an inner part and Ag atoms on the surface of the clusters (Fig. 11).

Another quantity that can give information on stability of a given cluster is the excess energy. Thereby, the total energy of the mixed  $\text{Ag}_m\text{Rh}_n$  cluster is compared with those of the pure Ag and Rh systems. Here, however, the choice of the pure reference systems is not obvious and one may suggest using the isolated atoms, the pure crystals, or finite clusters. We will here consider the two last suggestion. When comparing with the finite clusters, we shall consider clusters with the same total number of atoms in order to reduce the effects of having different surfaces. Accordingly, we define one excess energy according to

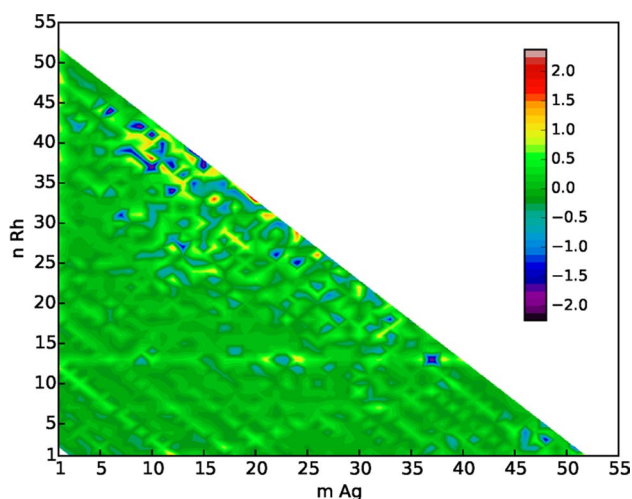


**Fig. 9** The stability function (in eV) according to Eq. (11) of the mixed  $\text{Ag}_m\text{Rh}_n$  clusters

$$E_{\text{ex},1}(m, n) = E_{\text{tot}}(m, n) - \frac{m}{m+n} E_{\text{tot}}(m+n, 0) - \frac{n}{m+n} E_{\text{tot}}(0, m+n) \quad (12)$$

and another one according to

$$E_{\text{ex},2}(m, n) = [E_{\text{tot}}(m, n) - m\bar{E}_{\text{tot}}(\infty, 0) - n\bar{E}_{\text{tot}}(0, \infty)] / (n+m)^{2/3} \quad (13)$$

with  $\bar{E}_{\text{tot}}(\infty, 0)$  and  $\bar{E}_{\text{tot}}(0, \infty)$  being the total energy per atom of the pure Ag and Rh crystals, respectively. Since the area of the surface for the clusters scale as  $(n+m)^{2/3}$ , we divide by this number in Eq. (13) in order to remove the size dependence of the surface contributions.

The resulting excess energies are shown in Fig. 10. The excess energy according to Eq. (13) is always positive, implying that the crystalline materials are more stable than the finite clusters, which can be related to the surface energies. The importance of the surface energies decreases with increasing cluster size. Moreover,  $E_{\text{ex},2}(m, n)$  is most positive for Rh-rich clusters. The fact that the cohesive energy of crystalline Rh is much larger than that of crystalline Ag [16] is most likely the explanation for this finding.

Also  $E_{\text{ex},1}(m, n)$  is in most case positive, suggesting that the pure clusters are more stable than the mixed ones. An exception is found for some Ag-rich and Rh-poor clusters. Thus, the admixture of a smaller part of Rh to Ag clusters seems to stabilize the mixed clusters. Those clusters that according to  $E_{\text{ex},1}(m, n)$  are most stable (i.e., have most negative values) are listed in Table 1. It is seen that these are all having structural motifs derived from the icosahedra. Moreover, the largest ones listed in the table have an Rh-containing icosahedron as a core with a shell of Ag atoms.

In order to illustrate the different structures that have been obtained in the present study for the mixed  $\text{Ag}_m\text{Rh}_n$  clusters, we shall discuss the case of  $m+n=34$ . When the

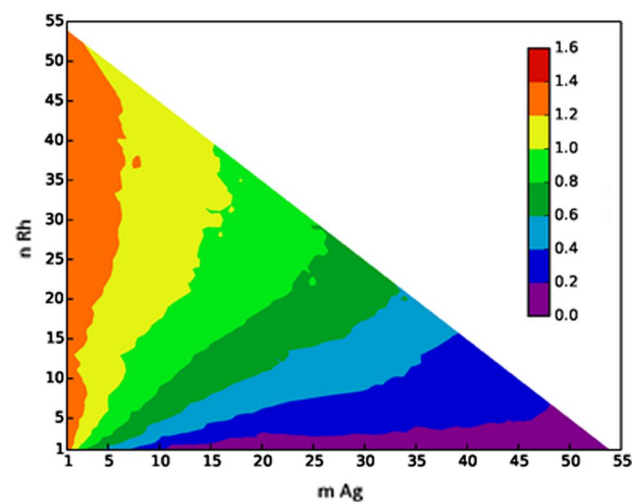
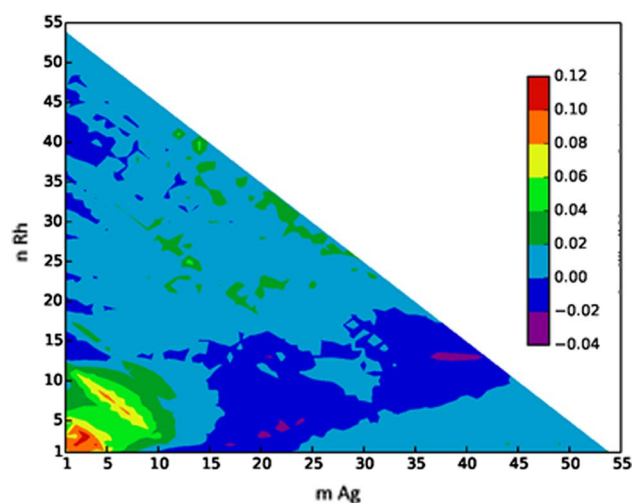


**Fig. 10** The excess energy according to Eqs. (12) and (13) for the mixed  $\text{Ag}_m\text{Rh}_n$  clusters when comparing with (upper part) the pure clusters and (lower part) the crystalline elements

total number of atoms is constant, as in this case, one may consider the stability function of Eq. (11) or, alternatively

$$\Delta'_2(n, m) = E_{\text{tot}}(m+1, n-1) + E_{\text{tot}}(m-1, n+1) - 2E_{\text{tot}}(m, n). \quad (14)$$

For  $m+n=34$ ,  $\Delta_2(n, m)$  of Eq. (11) has maxima for  $n=7, 13,$  and  $25$ , whereas  $\Delta'_2(n, m)$  of Eq. (14) has maxima for  $n=7, 13,$  and  $18$ . Thus, both similarities and differences are seen, implying that the concept of stability is not very easily defined for clusters with more than one type of atoms.

The four clusters with 34 atoms in total and of particularly high stability are shown in Fig. 11.  $\text{Ag}_{27}\text{Rh}_7$  contains a pentagonal bipyramid of Rh atoms covered by Ag atoms that have an anti-Mackay arrangement. The latter is also the case for  $\text{Ag}_{21}\text{Rh}_{13}$  although in this case, the Rh atoms form a p1h structure with a single Rh atom in the center. In

**Table 1** The most stable mixed  $\text{Ag}_m\text{Rh}_n$  clusters with  $E_{\text{ex},1}(m, n)$  less than  $-0.02$  eV/atom

$m + n$	$(m, n)$	Motif
12	(11, 1)	Ih <sub>13</sub> (f)
13	(12, 1)	Ih <sub>13</sub>
14	(13, 1)	Ih <sub>13</sub> + Ag
19	(17, 2)	pIh <sub>2</sub>
23	(20, 3)	pIh <sub>3</sub>
24	(21, 3)	pIh <sub>3</sub>
26	(22, 4)	pIh <sub>4</sub>
27	(22, 5)	pIh <sub>5</sub>
29	(24, 5)	pIh <sub>5</sub>
33	(20, 13)	pIh <sub>1</sub> aM
34	(21, 13)	pIh <sub>2</sub> aM
50	(37, 13)	Ih <sub>55</sub> (f)
51	(38, 13)	Ih <sub>55</sub> (f)
52	(39, 13)	Ih <sub>55</sub> (f)
53	(40, 13)	Ih <sub>55</sub> (f)
54	(41, 13)	Ih <sub>55</sub> (f)
55	(42, 13)	Ih <sub>55</sub>

The structural motifs are the 13- and 55-atomic icosahedra (Ih<sub>13</sub> and Ih<sub>55</sub>, respectively, partly only fragments of them (f). aM marks anti-Mackay icosahedra, and pIh<sub>k</sub> marks polyicosahedra

all cases, also for  $\text{Ag}_{16}\text{Rh}_{18}$  and  $\text{Ag}_9\text{Rh}_{25}$ , the Ag atoms are found in the outer regions of the cluster. For  $\text{Ag}_{16}\text{Rh}_{18}$ , the Rh atoms form a pIh structure, but for  $\text{Ag}_9\text{Rh}_{25}$  they form a part of the Ih<sub>55</sub> structure.

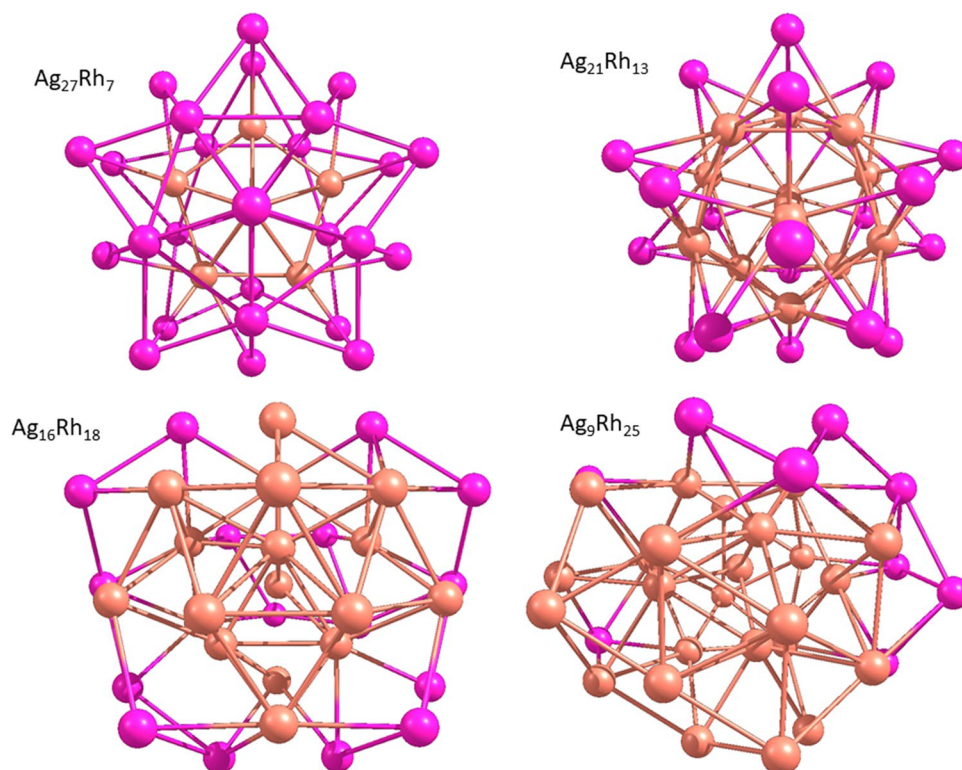
We finally mention that structures like  $\text{Ag}_{27}\text{Rh}_7$  and  $\text{Ag}_9\text{Rh}_{25}$  also were found by Rapallo *et al.* as particularly stable clusters in their theoretical study on other bimetallic clusters with a total of 34 or 38 atoms [15].

Next, we shall return to the structural properties of the mixed clusters and in particular focus on whether segregation or mixing is observed. A parameter that can quantify this is the so-called bond-order parameter that in our cases becomes

$$\sigma = \frac{N_{\text{Ag-Ag}} + N_{\text{Rh-Rh}} - N_{\text{Ag-Rh}}}{N_{\text{Ag-Ag}} + N_{\text{Rh-Rh}} + N_{\text{Ag-Rh}}} \quad (15)$$

with  $N_{\text{A-B}}$  being the number of A-B bonds. In our case, we consider two atoms as being bonded if their interatomic distance is below 3.1 Å.  $\sigma$  approaches +1 (−1) in case of complete segregation (mixing). This function is shown in Fig. 12. It is seen that it is almost always positive, indicating some tendency towards segregation.

Finally, we shall study the segregation in more details. To this end, we define at first the center of a mixed  $\text{Ag}_m\text{Rh}_n$  cluster,

**Fig. 11** Schematic representation of some selected  $\text{Ag}_m\text{Rh}_n$  clusters for  $m + n = 34$ . Pink and orange spheres represent Ag and Rh atoms, respectively

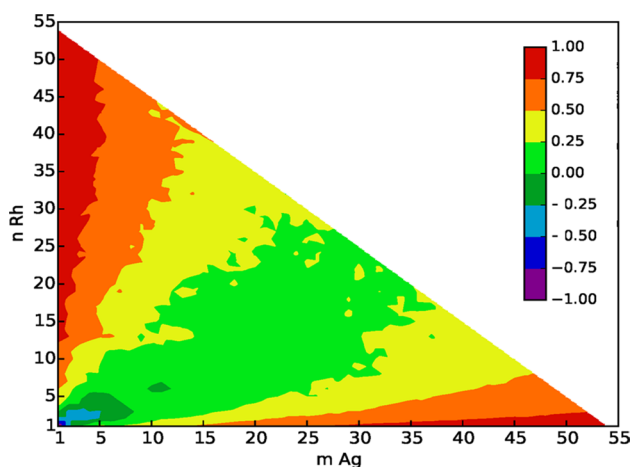


**Fig. 12** The bond order parameter according to Eq. (15) for the mixed  $\text{Ag}_m\text{Rh}_n$  clusters

$$\vec{R}_0 = \frac{1}{m+n} \sum_i \vec{R}_i \quad (16)$$

where  $\vec{R}_i$  is the position of the  $i$ th atom in the cluster. Subsequently, we define an averaged radial distance for the Ag and Rh atoms in the mixed cluster,

$$\begin{aligned} \langle r_{\text{Ag}} \rangle &= \frac{1}{m} \sum_i' |\vec{R}_i - \vec{R}_0| \\ \langle r_{\text{Rh}} \rangle &= \frac{1}{n} \sum_i' |\vec{R}_i - \vec{R}_0| \end{aligned} \quad (17)$$

where the two summations run over only the Ag or Rh atoms, respectively. The ratio

$$x_{\text{seg}} = \frac{\langle r_{\text{Rh}} \rangle}{\langle r_{\text{Ag}} \rangle} \quad (18)$$

is close to 1 if the two elements are mixed and  $> 1$  ( $< 1$ ) if the Rh atoms are mainly in the outer (inner) region.

This ratio is shown in Fig. 13. It is clear that it is constantly  $< 1$ , implying that Rh forms a core with Ag atoms forming a shell. That this is the case is in agreement with the general criteria for such structures [2]: the larger cohesive energy [16] and surface energy [17] together with the smaller size of the Rh atoms (cf. Fig. 2) make Rh prefer to occupy the inner part of the clusters with Ag forming a shell.

## 4 Conclusions

In the present work, we have studied the properties of mixed Ag–Rh nanoalloys. In the macroscopic case, the solubilities of Ag in Rh and of Rh in Ag are very different, which makes it very difficult to predict the properties of the nanoalloys

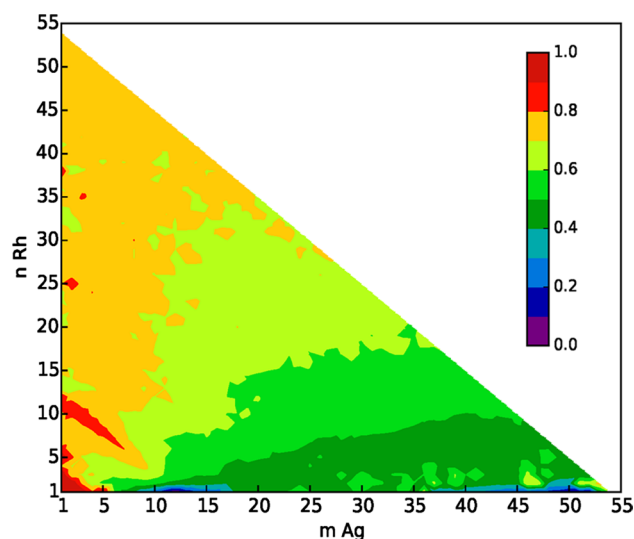


**Fig. 13** The segregation parameter of Eq. (18) for the mixed  $\text{Ag}_m\text{Rh}_n$  clusters

who have sizes below that of the thermodynamic limit and for which surface effects are expected to be dominating.

We studied all stoichiometries with up to 55 atoms giving in total more than 1500 different mixed clusters. An unbiased structure optimization for all these systems using accurate electronic-structure methods is not possible. Instead, we used an approximate method to describe the interatomic interactions, i.e., the many-body Gupta potential, in combination with genetic algorithms for the unbiased structure optimization.

An obvious outcome of the calculations is the structures and energies of the more than 1500 clusters. A next challenge is, therefore, to extract useful information from this large amount of data. To this end, we applied various descriptors, most notably a similarity function that can quantify structural similarity between two objects. With this, we found that the structures of the pure clusters are quite similar for clusters with up to around 20 atoms. Moreover, there was some tendency for the mixed clusters to show a higher similarity with the pure Rh clusters of the same size than with the pure Ag clusters. Moreover, we could also use this concept to demonstrate a strong similarity with the 55-atomic icosahedron for most clusters with the exception of those with  $m \simeq n$  or  $m+n \simeq 20-30$ . Other descriptors, i.e., the average effective coordination number, the bond order parameter, and a segregation parameter all indicate some degree of segregation with Rh atoms forming a core and Ag atoms forming a shell.

An excess energy based on comparing the energies of the clusters with those of the crystalline systems suggests that the clusters are less stable than the crystalline systems, a finding that can be explained through the large surface



effects for the clusters. This excess energy is, moreover, most positive for the Rh-rich and Ag-poor systems since the cohesive and surface energies of Rh are much larger than those of Ag. A stability function for identifying particularly stable cluster sizes when comparing with neighboring sizes predicts that in particular four clusters, all with 34 atoms in total, are particularly stable. These clusters have high symmetry, which is a part of the explanation for this finding.

We hope that we have demonstrated that bimetallic clusters indeed have their own properties and not just some kind of average of those of the pure monatomic clusters. Moreover, by comparing with our earlier studies on  $Ni_mAg_n$  and  $Cu_mAg_n$  clusters [18, 19] we can also see that different bimetallic nanoalloys have different properties. For instance, even though we find similar structural elements for the different bimetallic nanoalloys,  $A_mB_n$ , for different metals (A,B) the same stoichiometries ( $m, n$ ) have in most cases different structures.

**Funding** Open Access funding enabled and organized by Projekt DEAL.

### Compliance with ethical standards

**Conflict of interest** The authors declare that they have no conflict of interest.

**Open Access** This article is licensed under a Creative Commons Attribution 4.0 International License, which permits use, sharing, adaptation, distribution and reproduction in any medium or format, as long as you give appropriate credit to the original author(s) and the source, provide a link to the Creative Commons licence, and indicate if changes were made. The images or other third party material in this article are included in the article's Creative Commons licence, unless indicated otherwise in a credit line to the material. If material is not included in the article's Creative Commons licence and your intended use is not permitted by statutory regulation or exceeds the permitted use, you will

need to obtain permission directly from the copyright holder. To view a copy of this licence, visit <http://creativecommons.org/licenses/by/4.0/>.

### References

1. Knight WD, Clemenger K, de Heer WA, Saunders WA, Chou MY, Cohen ML (1984) *Phys Rev Lett* 52:2141–2143
2. Ferrando R, Jellinek J, Johnston RL (2008) *Chem Rev* 108:845–910
3. Jellinek J, Krissinel EB (1996) *Chem Phys Lett* 258:283–292
4. Jellinek J, Krissinel EB (1999) In: Jellinek (ed.) *Theory of atomic and molecular clusters with a glimpse at experiments*. Springer, Heidelberg
5. Christensen A, Ruban AV, Stoltze P, Jacobsen KW, Skriver HL, Nørskov JK, Besenbacher F (1997) *Phys Rev B* 56:5822–5834
6. Rossler H (1900) *Chem Ztg* 2:733–735
7. Rudnitskii AA, Khotinskaya AN (1959) *Russ J Inorg Chem* 4:1053–1056
8. Kohaut S, Springborg M (2016) *J Clust Sci* 27:913–933
9. Gupta RP (1981) *Phys Rev B* 23:6265–6270
10. Rosato V, Guillope M, Legrand B (1989) *Phil Mag* 59:321–336
11. Cleri F, Rosato V (1993) *Phys Rev B* 48:22–33
12. Deaven DM, Ho KM (1995) *Phys Rev Lett* 75:288–291
13. Kohaut S, Thiel P, Springborg M (2017) *Comput Theo Chem* 1107:30–48
14. Hoppe R (1979) *Z Kristallogr* 150:23–52
15. Rapallo A, Rossi G, Ferrando R, Fortunelli A, Curley BC, Lloyd LD, Tarbuck GM, Johnston RL (2005) *J Chem Phys* 122:194308
16. Turchanin MA, Agraval PG (2008) *Powder Metall Metal Ceram* 47:26–39
17. Skriver HL, Rosengaard NM (1992) *Phys Rev B* 46:7157–7168
18. Molayem M, Grigoryan VG, Springborg M (2011) *J Phys Chem C* 115:7179–7192
19. Molayem M, Grigoryan VG, Springborg M (2011) *J Phys Chem C* 115:22148–22162

**Publisher's Note** Springer Nature remains neutral with regard to jurisdictional claims in published maps and institutional affiliations.